SUPPLEMENTARY INFORMATION

Intention and Attention: Different functional roles for LIPd and LIPv

Liu YQ, Yttri EA and Snyder LH.

Speed-accuracy trade-off of control and injection data. Lesions could potentially affect both reaction time and error rate. To determine whether we could combine these two effects into a single performance measurement, we binned contralateral hemifield data from control sessions (n = 236) by error rate and plotted each bin's mean RT (**Supplementary fig. 2**). We did this for both saccade and search tasks.

The saccade control data showed a clear inverse relationship, commonly referred to as a speed-accuracy trade-off [1-3], that was well-described by a linear function (slope = –0.94 ms per % error; Pearson's correlation coefficient r = –0.97 [P = 0.0002]; **Supplementary fig. 2a**, black). We therefore combined saccade RT and error rate into a single "adjusted RT" measurement by extrapolating the data to the y-intercept using the slope of the speed-accuracy trade-off (adjusted RT = RT – slope × error rate). This is equivalent to asking what RT would have been observed in a given session if the speed-accuracy trade-off had been adjusted for zero errors.

A similar speed-accuracy trade-off can also be seen in the saccade LIPv injection data (slope = –1.3 ms per %; Pearson's correlation coefficient r = –0.7 [P = 0.001]; **Supplementary fig. 2d**, green), and in the LIPd injection data (slope = –0.45 ms per %; Pearson's correlation

coefficient r = –0.42 [P = 0.096]; **Supplementary fig. 2c**, green). A majority of the LIPd and LIPv data points lie above the control trade-off line (**Supplementary fig. 2c and d**), indicating impaired saccadic performance (an increase in RT or errors or both) after lesions. The slope of the trade-off in LIPd appears to be affected by the lesions, but the number of data points is low and the reduction is not significant (P = 0.22, Student's t-test on the coefficients of the two linear models). The same is true for the intercept of the post-lesion trade-off in LIPv (P = 0.11).

The visual search data (n = 227) showed a different pattern. Search RT was an increasing, saturating function of search error rate (**Supplementary fig. 2b**). Although the data could be fit to a straight line (r = 0.86, P = 0.013), error rates were associated with little change in RT (0.12 ms per %, P = 0.013). Furthermore, the two effects covaried rather than opposed one another. Thus there was no evidence for a speed-accuracy trade-off in search, and as a result, we did not combine error rate and RT for search.

No evidence for cumulative lesions

To test for potential long-term damage caused by repeated injections, we plotted lesion effects as a function of time (**Supplementary fig. 3**). Data from LIPd (**Supplementary fig. 3**, circle) and LIPv (**Supplementary fig. 3**, square), from the contralateral (saccade in green and search in red) and ipsilateral (black) hemifields, from the saccade (left) and search (right) tasks, and from each animal are all plotted separately as a function of session number. Inspection of the data reveals no obvious trends. This was confirmed using two-factor ANCOVA (continuous variable: session number; factors: laterality and area). Six separate ANCOVAs were performed on the search and saccade data from each animal. In every case the main effect of time (session number) was associated with a P value greater than 0.14, and there were no significant

interactions involving time, indicating that there was no cumulative lesion effect in either task. The main effect of laterality was significant for saccades in two animals (Q and G) and for search in one animal (G).

Measurements of injection depth do not assume equal spread of manganese and muscimol

In each of our lesion experiments, we co-injected muscimol and manganese (Mn), and measured the injection depth as the Euclidean distance from the center of Mn halo to the gyral surface adjacent to the intraparietal sulcus. These depth measurements, along with the rest of our analysis, are completely independent of the relative rates at which muscimol and Mn spread. On the one hand, muscimol and Mn have very different molecular weights and may have different binding affinities for water, and therefore are likely to diffuse at different rates in the brain. On the other hand, the initial dispersion of the injected volume may occur by convection (bulk flow) rather than diffusion. In this case, the spread of muscimol and Mn would likely be similar. Since we do not know whether convection or diffusion dominates, we were careful not to have any of our measurements depend in any way on the relative rates or extent of muscimol and manganese spread. We only assume that the center of the Mn halo matches the center of the muscimol inactivation. Our preliminary unit recordings following muscimol+Mn injections (data not shown) were consistent with both this assumption and the data of Arikan et al. on symmetric muscimol spread[4]. Our lesion overlap map (**Fig. 5**) was generated based on the center of the Mn halo in our injection MRIs and the muscimol spread data of Arikan et al., and not by inspection of the MR halo size. Thus, none of our conclusions depends on the degree of correspondence between muscimol and Mn spread.

Interpretation of a negative finding of search effect in LIPd

We interpret our results to mean that both LIPd and LIPv are involved in saccade control, and that LIPv (but not LIPd) is involved in attentional control. The argument that LIPd is not involved in attention comes about because of a negative finding, that injections in LIPd do not affect the search task. Negative findings are difficult to interpret in inactivation experiments. However, the effect on saccades in LIPd provides evidence that the LIPd injections were successful, that is, it provides a positive control for the lack of an LIPd search effect. Lesions in LIPv and LIPd had comparable effects on saccades, suggesting that the muscimol lesions in the two areas were in some sense equally efficacious in inactivating the cortex. In the light of the equal effects of LIPd and LIPv lesions on saccades, the fact that the LIPv lesions impaired visual search provides another control for the lack of an LIPd effect on search. Thus, although the argument that LIPd is not involved in attention comes about because of a negative finding, it is a negative finding accompanied by strong controls.

Consistent effects across the rostrocaudal extent of the lateral bank of the IPS

To examine the consistency of the lesion effects along the caudal/posterior to rostral/anterior extent of LIP, we measured the absolute distance from the center of the manganese halo to the junction of IPS and POS (parietal occipital sulcus) in the horizontal plane of each injection MRI. We then computed the normalized anterior-to-posterior distance (AP') relative to the full anterior-to-posterior length of the IPS, defined such that the rostral/anterior end of the sulcus has an AP' of 1 and the caudal/posterior end has an AP' of 0 (see Methods). We plotted the LIPd and LIPv lesion effects on saccade (**Supplementary fig. 5a and b**, green) and search (**Supplementary fig. 5c and d**, red) as a function of AP'. Saccade and search effects were

similar across the AP' range that we tested (0.22 to 0.55) in both LIPd (**Supplementary fig. 5**, **left, a and c**) and LIPv (**Supplementary fig. 5, right, b and d**). There was no significant linear trend (least-squares regression fit) in any of the data (slopes not significantly different from zero: P = 0.74 for saccade effect in LIPd, P = 0.12 for search effect in LIPd, P = 0.51 for saccade effect in LIPv, and P = 0.12 for search effect in LIPv). It is important to note that only a relatively small anterior-posterior extent was tested, however.

Single unit recording studies suggest a rough topography in LIP[5, 6]. The lower visual field may be represented more anteriorly and the upper visual field more posteriorly[5, 6]. To examine the topography of impairment after LIP lesions, we determined the target direction associated with the strongest lesion effect. We refer to this as the best direction of the lesion. We then plotted the best direction of saccade and search lesions as a function of AP' (**Supplementary fig. 6**). Within the one-third of the sulcus that we studied, the downward direction was slightly emphasized in the posterior/caudal portion of the sulcus, and the upper field was slightly emphasized in the anterior/rostral portion. This is opposite to the gradient reported by Blatt et al.[6] and Ben Hamed et al.[5].

Lesion effects on saccade metrics and duration

Saccades **accuracy** was largely unaffected after LIPd or LIPv injections. Mean saccade amplitude was unchanged (P >= 0.15) for all but one direction in LIPd (–0.41 deg, P = 0.029; **Supplementary fig. 7a**). This was also true when pooling amplitude across all directions (LIPd: mean effect = 0.04º [P = 0.62, two-sided paired permutation test]; LIPv: mean effect = –0.02º [P = 0.84]). Saccade **precision** was largely unaffected as well. The standard deviation of saccade amplitude was unchanged (P >= 0.15) for all but one direction in both LIPd and LIPv

(**Supplementary fig. 7c and d**). When pooled across all directions, the standard deviation of saccade amplitude increased slightly after LIPv lesions (+0.19º [P = 0.003]) but not after LIPd lesions (+0.04º [P = 0.76]). Similarly, saccade **duration** was unchanged (P >= 0.15) for six of eight directions in each area (**Supplementary fig. 7f**). When pooled across all directions, saccade duration decreased slightly after LIPd lesions (mean effect = –0.83 ms [P = 0.02]) and after LIPv lesions (mean effect = –0.64 ms [P = 0.04]). Similar results were obtained in each animal when considered separately (see **Supplementary Table 1** for individual monkey data).

LIPd and LIPv lesions do not affect foveal stability

Previous studies have proposed that LIPd may play a greater role in eye fixation than LIPv[5, 7]. We therefore compared the rate of fixation errors in the memory saccade task before and after injections into LIPd and LIPv to test the hypothesis that LIPd injections would impair fixation to a greater extent than LIPv injections. Fixation errors occurred in 3.4% of trials in control sessions (n = 35). The rate slightly but significantly increased in the whole visual field by 1.4% (P = 0.01, two-sided permutation test) after LIPd injections and by 1.0% (P = 0.05) after LIPv injections. The increased error rates in the two areas were not significantly different from one another (P = 0.5). This was also true when individual directions were considered separately (two-way [area × direction] ANOVA on lesion effect, main effect of area: F(1) = 1.4, P = 0.24; **Supplementary fig. 8**). These data do not support the hypothesis that LIPd and LIPv play different roles in fixation.

Anatomical lesion overlap map. The image was registered to a stereotaxically-oriented template image computed from the mean of several fascicularis macaque T1-weighted brain

MRIs (sum database: F6 atlas) using a 12 parameter affine registration algorithm[8]. In-house software then corrected for intensity non-uniformity within the brain introduced by the spatial signal-to-noise characteristics of the RF coil and magnetic field. Occasionally, images severely compromised by the titanium head post needed additional masking-out of distorted regions to improve the quality of the alignment. The center of each lesion was measured from the MRI. The inactivation is not confined to the point of the injection, but spreads several millimeters in all directions[4]. Therefore the inactivation radius was estimated, based on the injection volume and published data regarding muscimol effective spread, as a sphere with a diameter of 3 milimeters, times the cube root of the volume in microliters[4]. These idealized lesion volumes were sorted based on effect and then projected onto a 3-D volume of one of the two fascicularis monkeys' brains, whose cortical surface had been created by segmenting the gray and white matter of the monkey's own aligned MPRAGE[9], using automated segmentation tool. The 3-D lesion volume maps were thresholded at 20% (i.e., only voxels covered by at least 20% of the effective injections were shown; **Fig. 5a and b**). An image of the difference between Figs. 5a and b, without thresholding, was then projected onto a 2-D semi-inflated cortical surface (**Fig. 5c)**.

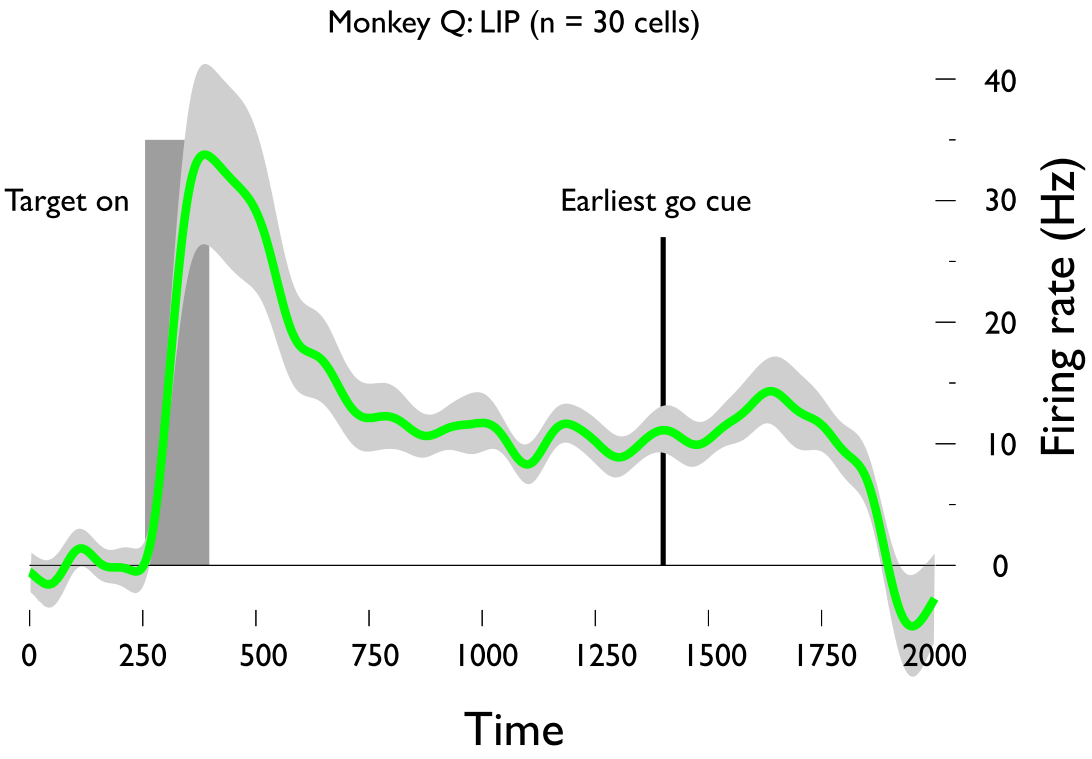

Supplementary figure 1 | Single unit responses across all LIP neurons. Prior to performing any injections, area LIP was mapped out using functional criteria in each animal. These criteria included brisk responses to a target onset and sustained activity during a memory period. Tracks containing a high percentage of such cells were considered to cross LIP. The averaged time course of memory saccade trial activity from 30 LIP cells in one monkey is shown.

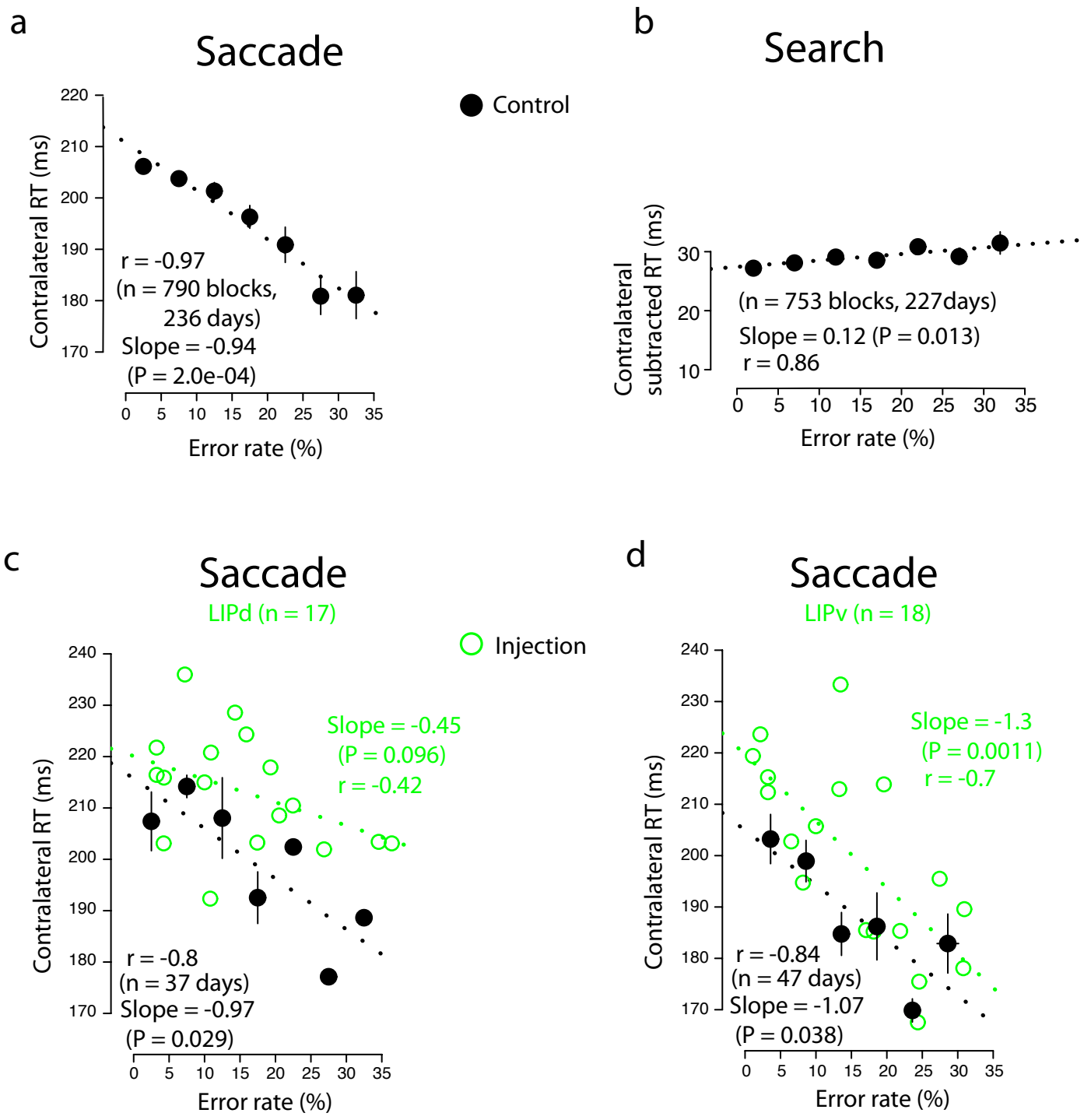

Supplementary figure 2 | Speed-accuracy trade-off of control and injection data. a & b. Three monkey's contralateral average saccade RTs and search subtracted RTs (trials with distractors minus trials without distractors) from control session saccade (a) and search (b) tasks, plotted against error rate. Blocks of control data (approximately 40 trials each) were sorted into 5% error rate bins. c & d, Three monkeys' contralateral average saccade RTs from control sessions (black) and injection sessions (green), plotted against saccade error rates for LIPd (c) and LIPv (d). Sessions of control data (approximately 240 trials each) were sorted into 5% error rate bins. Two injection data points were shifted slightly to avoid overlap in both panels c & d. Error bars are one standard error of the average control RT (y) and error rate (x) for that bin (sometimes smaller than the diameter of the data point). The black and green dotted lines are least-squares regression fits for the control and injection data, respectively.

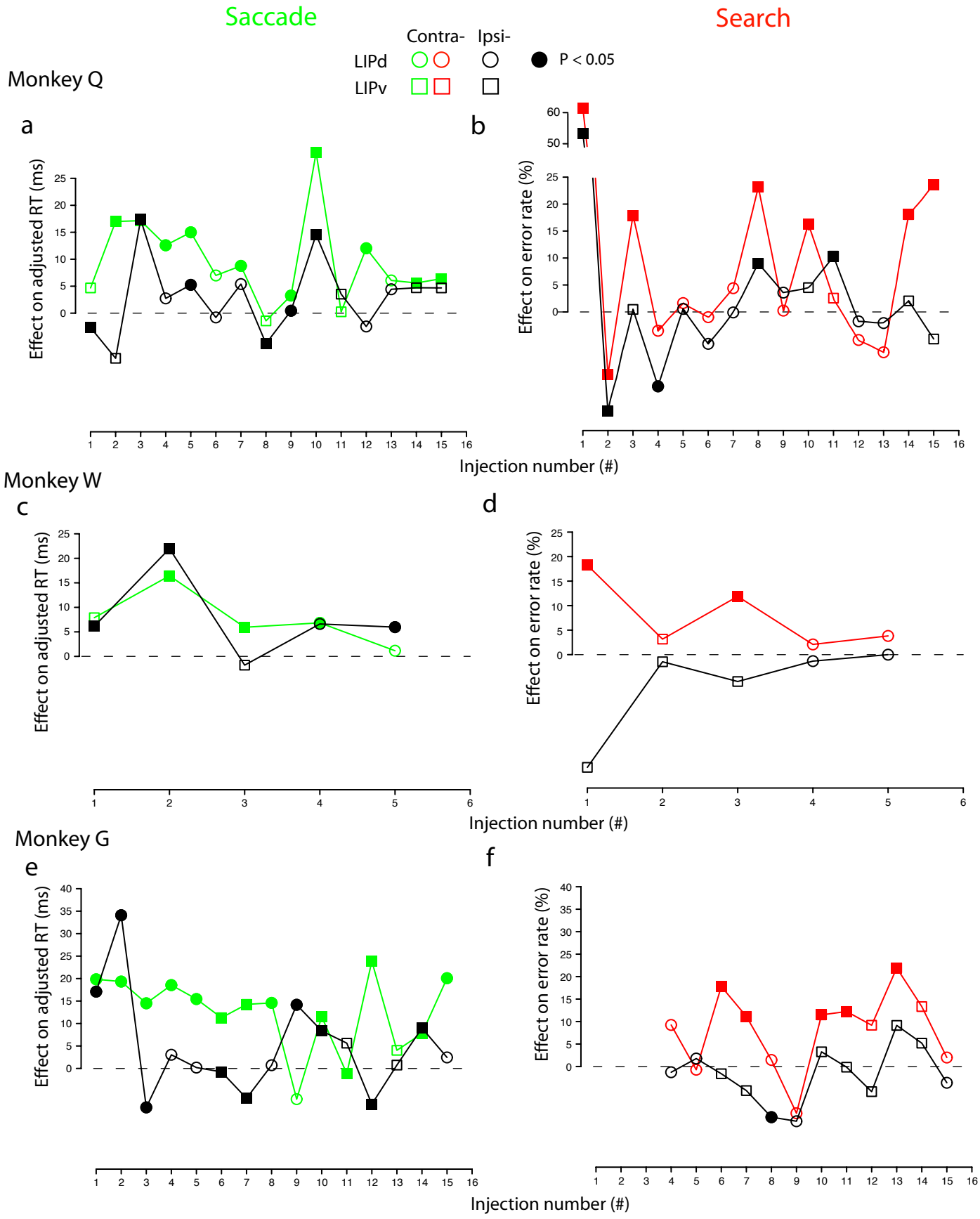

Supplementary figure 3 | LIP lesion effects as a function of time. Data from LIPd (circles) and LIPv (squares), from the contralateral (saccade in green and search in red) and ipsilateral (black) hemifields, from saccade (left) and search (right) tasks, and from each animal, plotted separately as a function of session number (chronologically ordered). Filled circles or squares represent significant lesion effects. See text for significance tests.

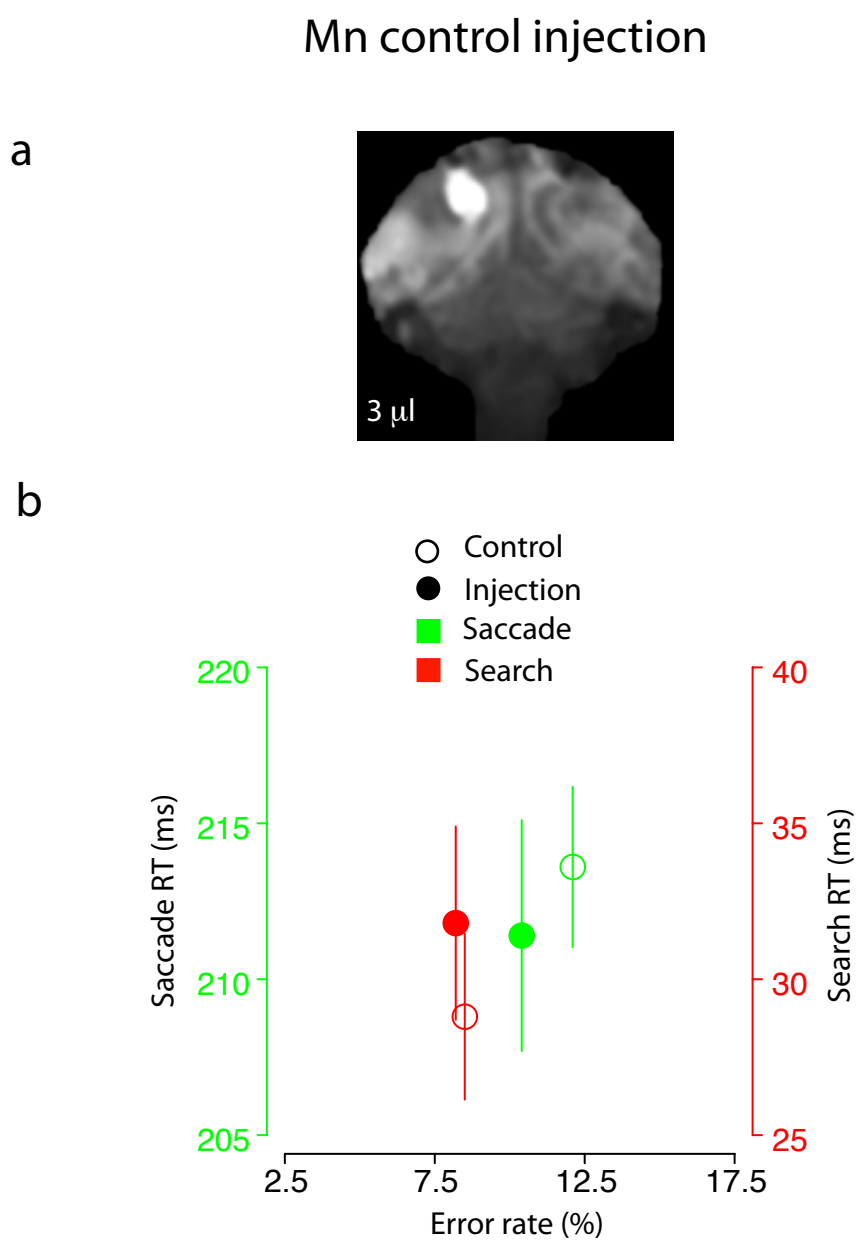

Supplementary figure 4 | MRI and task performance of a manganese control injection. a. Manganese alone injection (3 µl, without muscimol mixed in) resulted in a bright halo in the dorsal and ventral portions of lateral and medial banks of the IPS, seen in a a coronal slice. b. The mean of saccade (green) and search (red) RTs from this injection (solid circles) and its matched controls (hollow circles) are plotted against their corresponding error rates. Neither RTs nor error rates were affected by this manganese control injection.

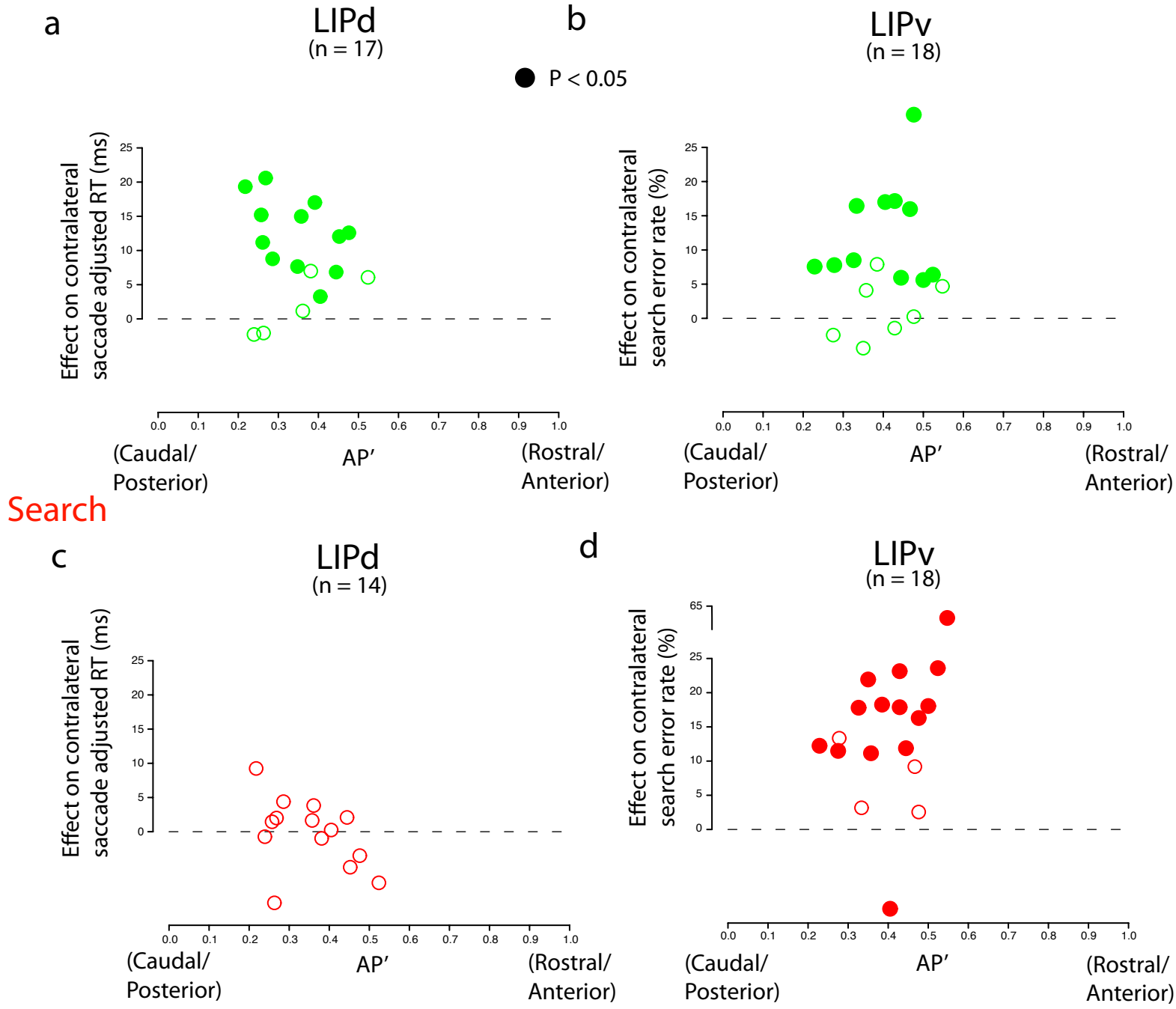

Supplementary figure 5 | Lesion effects along the caudal (posterior) to rostral (anterior) extent of LIPd and LIPv. LIPd (left, a & c) and LIPv (right, b & d) lesion effects on saccade (top, a & b, green) and search (bottom, c & d, red), plotted against normalized anterior-to-posterior distance (AP'; see methods). There was no significant linear trend in any of the data shown here.

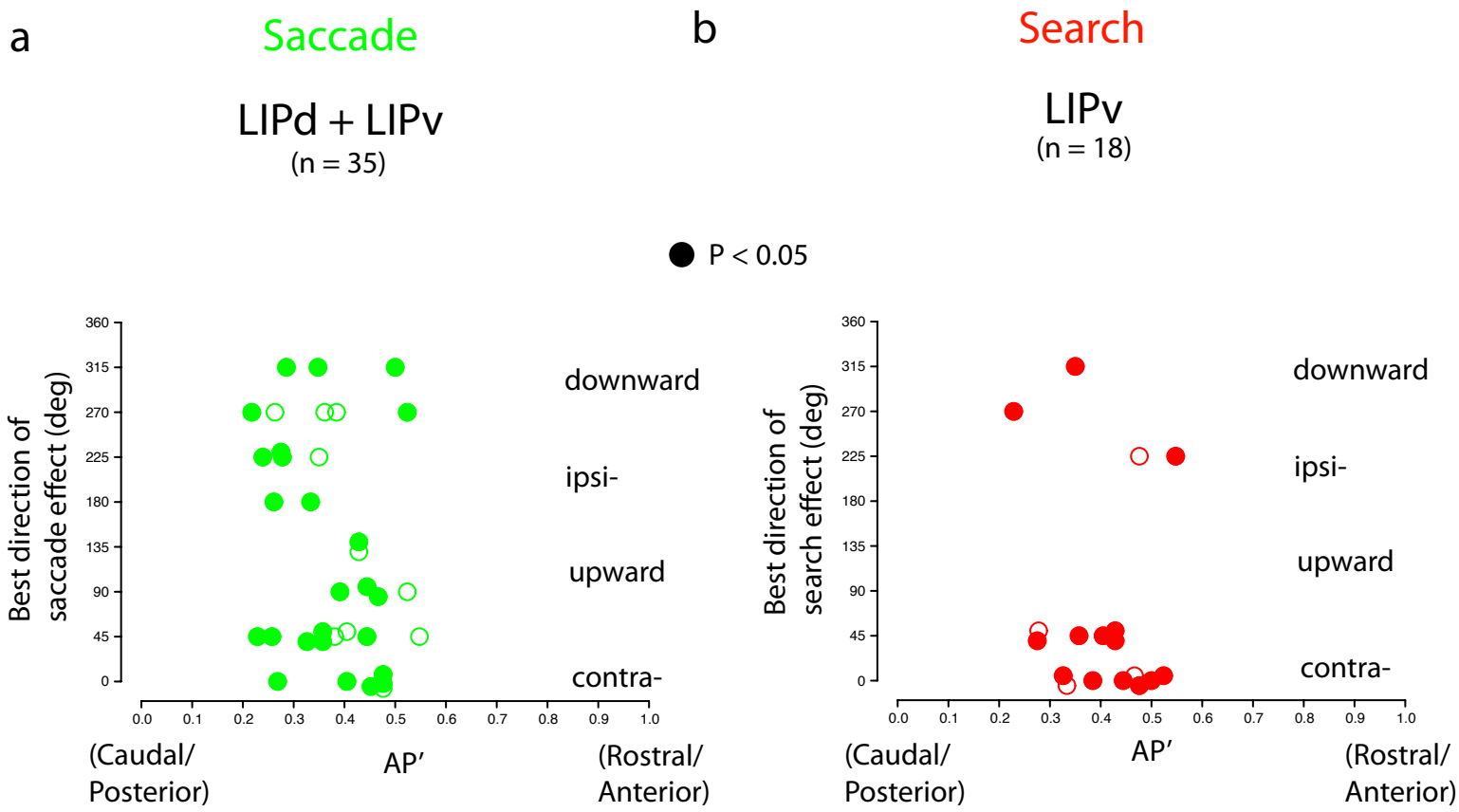

Supplementary figure 6 | Best lesion directions along the caudal (posterior) to rostral (anterior) extent of LIP. Target directions in which lesion effects on saccade adjusted RT (a, green) and search error rate (b, red) were strongest, as a function of normalized anterior-to-posterior distance (AP'). Some data points were shifted slightly vertically to avoid overlap. LIPd and LIPv lesion effects on saccade were not significantly different, and thus are combined in a. Only LIPv but not LIPd lesions impaired search, and therefore only LIPv injection data are shown in b. 45º to 135º correspond to upper field directions, 225º to 315º correspond to lower field directions, and 0º, 45º and 315º correpond to the three contralateral directions tested. No substantial anteroposterior gradient for the visual field representation was seen.

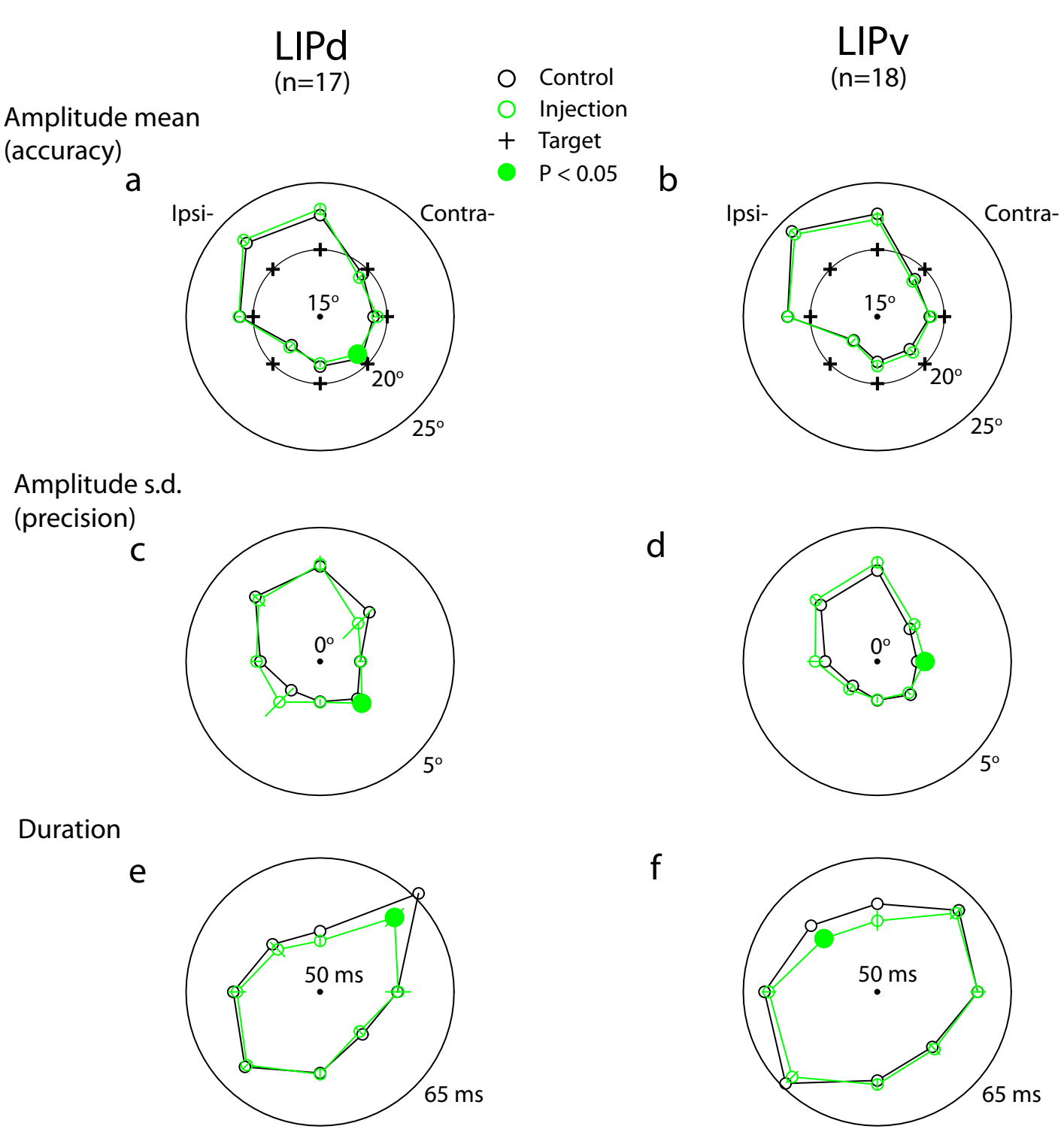

Supplementary figure 7 | Effects of LIPd and LIPv inactivations on memory-guided saccade metrics and duration. a & b, Mean saccade amplitude (accuracy) from the control (black) and inactivation (green) trials, plotted by target direction, for LIPd (a) and LIPv (b). The center of the circles indicates a 15° displacement from the fixation point. Target locations, marked as crosses (+) along the inner circle, were 20° away from the fixation point. c & d, Standard deviation (s.d.) of the saccade amplitude (precision) for the control data (black) and the inactivation data (green), plotted by target direction, for LIPd (c) and LIPv (d). e & f, Mean saccade duration from the control (black) and inactivation (green) trials, plotted by target direction, for LIPd (e) and LIPv (f). The center of the circles indicates 50 ms movement duration. Error bars are ± 1 standard error of the difference between the controls and injections. Solid data points indicate significant effects following lesions ($P < 0.05$).

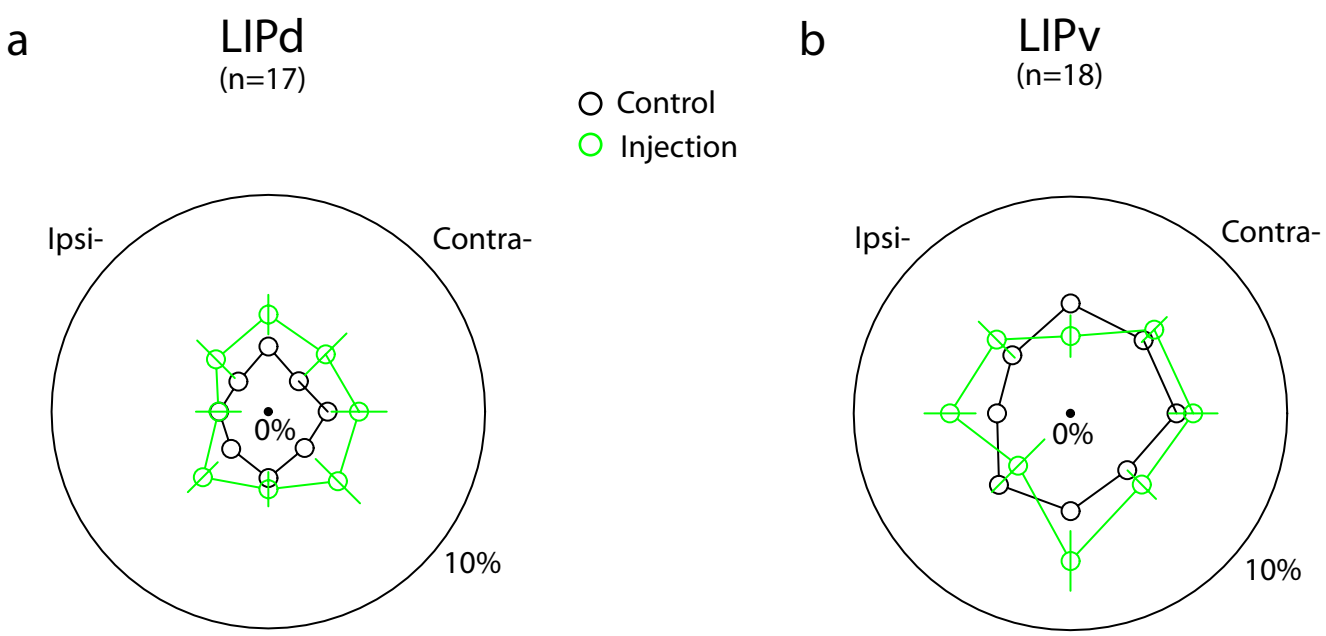

Supplementary figure 8 | Effects of LIPd and LIPv inactivations on saccade fixation errors.
a & b, Errors caused by eye movements occurring any time between the transient peripheral target presentation and the fixation point offset during memory-guided saccade trials are referred to as saccade fixation errors. Mean saccade fixation error rates of the control sessions (black) and injection sessions (green, a: LIPd; b: LIPv) are plotted by target direction. Outer circle indicates a 10% error rate. Error bars are ± 1 standard error of the difference between the controls and injections.

Single LIPv injection with/without leakage along the injection track

a

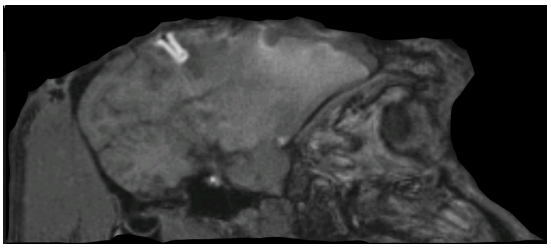

b

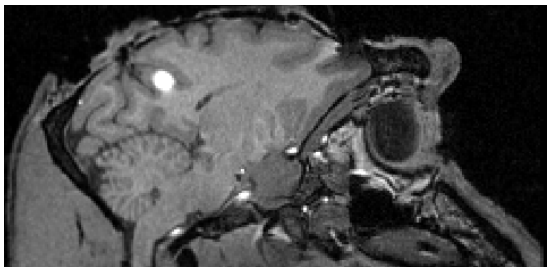

Supplementary figure 9 | MRIs of injections with and without leakage. a. An example injection that showed backfilling of the injectate during cannula retraction. A sagittal section is shown. This injection was rejected from our data set. b. A successful LIPv injection that did not show leakage and resulted in a well localized halo in the lateral bank of the IPS.

Supplementary Table 1. Effect of reversible lesions on saccade metrics and duration.

Contralateral lesion effects		Mean of G,Q & W	Monkey G	Monkey Q	Monkey W
Hypometria (degree)	LIPd	29% –0.16 ± 0.16	50% –0.24 ± 0.29	14% –0.21 ± 0.2	0% 0.35 ± 0.1
	LIPv	17% 0.06 ± 0.19	14% 0.25 ± 0.37	25% –0.29 ± 0.2	0% 0.57 ± 0.31
Precision (degree)	LIPd	29% –0.17 ± 0.35	38% –0.46 ± 0.74	29% 0.15 ± 0.11	0% –0.1 ± 0.15
	LIPv	17% 0.07 ± 0.12	14% 0.21 ± 0.16	13% –0.23 ± 0.17	33% 0.51 ± 0.27
Duration (ms)	LIPd	6% –1.42 ± 0.9	0% –1.23 ± 0.49	14% –1.95 ± 2.2	0% –0.32 ± 0.17
	LIPv	17% 0.03 ± 0.66	29% –0.12 ± 1.05	13% 0.2 ± 1.21	0% –0.07 ± 0.74

Entries show mean ± standard deviation (s.d.) of LIPd and LIPv lesion effects on saccade accuracy (hypometria), precision, and duration. The percentage are the proportion of sites that showed a significant impairment in the mean or standard deviation of contralaterally-directed saccade amplitude (decrease in mean and increase in s.d.), or a significant delay in the mean contralaterally-directed saccade duration ($P < 0.05$, two-sided Welch's t-test for RT comparison and two-sided F [variance ratio] test for s.d. comparison).

Supplementary Table 2. Behavioral deficits after LIPd and LIPv lesions and the effect of eye position on those deficits

	LIPd		LIPv	
	Saccade (ms)	Search (%)	Saccade (ms)	Search (%)
Post-lesion deficit	**11.1 ± 1.8**	–0.2 ± 1.4	**10.1 ± 2.0**	**15.7 ± 3.4**
Eye position effect	0.1 ± 2.5	1.6 ± 2.1	–2.0 ± 1.6	**11.4 ± 4.7**

Entries show mean ± s.e.m. of the reversible lesion effect on saccade adjusted RT and search error rate in LIPd and LIPv, and the effect of changing eye position from five degrees ipsilateral to five degrees contralateral. Bold font indicates significant effects ($P < 0.05$).

References

1. Meyer, D.E., Abrams, R.A., Kornblum, S., Wright, C.E., &Smith, J.E. *Optimality in human motor performance: ideal control of rapid aimed movements.* Psychol Rev. **95**, 340-70 (1988).
2. Plamondon, R. & Alimi, A.M. *Speed/accuracy trade-offs in target-directed movements.* Behav Brain Sci. **20**, 279-303; discussion 303-49 (1997).
3. Schmidt, R.A., Zelaznik, H., Hawkins, B., Frank, J.S., &Quinn, J.T., Jr. *Motor-output variability: a theory for the accuracy of rapid motor acts.* Psychol Rev. **47**, 415-51 (1979).
4. Arikan, R., et al. *A method to measure the effective spread of focally injected muscimol into the central nervous system with electrophysiology and light microscopy.* J Neurosci Methods. **118**, 51-7 (2002).
5. Ben Hamed, S., Duhamel, J.R., Bremmer, F., &Graf, W. *Representation of the visual field in the lateral intraparietal area of macaque monkeys: a quantitative receptive field analysis.* Exp Brain Res. **140**, 127-44 (2001).
6. Blatt, G.J., Andersen, R.A., &Stoner, G.R. *Visual receptive field organization and cortico-cortical connections of the lateral intraparietal area (area LIP) in the macaque.* J Comp Neurol. **299**, 421-45 (1990).
7. Ben Hamed, S. & Duhamel, J.R. *Ocular fixation and visual activity in the monkey lateral intraparietal area.* Exp Brain Res. **142**, 512-28 (2002).
8. Snyder, A.Z., *Difference image vs. ratio image error function forms in PET-PET realignment. In: Quantification of Brain Function Using PET* Vol. (ed. R. Myer, V.J.C., D.L. Bailey, and T. Jones.) (San Diego, CA, Academic Press, 1995).
9. Van Essen, D.C. *Windows on the brain: the emerging role of atlases and databases in neuroscience.* Curr Opin Neurobiol. **12**, 574-9 (2002).